On subregion action complexity in AdS_3 and in the BTZ black hole

Roberto Auzzi[a,b], **Stefano Baiguera**[c], **Andrea Legramandi**[c],
Giuseppe Nardelli[a,d], **Pratim Roy**[e] and **Nicolò Zenoni**[a,b]

[a] *Dipartimento di Matematica e Fisica, Università Cattolica del Sacro Cuore,*
Via Musei 41, 25121 Brescia, Italy

[b] *INFN Sezione di Perugia, Via A. Pascoli, 06123 Perugia, Italy*

[c] *Università degli studi di Milano-Bicocca and INFN, Sezione di Milano-Bicocca,*
Piazza della Scienza 3, 20161, Milano, Italy

[d] *TIFPA - INFN, c/o Dipartimento di Fisica, Università di Trento,*
38123 Povo (TN), Italy

[e] *School of Physical Sciences, NISER, Bhubaneshwar, Khurda 752050, India*

E-mails: roberto.auzzi@unicatt.it, s.baiguera@campus.unimib.it,
a.legramandi@campus.unimib.it, giuseppe.nardelli@unicatt.it,
proy@niser.ac.in, nicolo.zenoni@unicatt.it

Abstract

We analytically compute subsystem action complexity for a segment in the BTZ black hole background up to the finite term, and we find that it is equal to the sum of a linearly divergent term proportional to the size of the subregion and of a term proportional to the entanglement entropy. This elegant structure does not survive to more complicated geometries: in the case of a two segments subregion in AdS_3, complexity has additional finite contributions. We give analytic results for the mutual action complexity of a two segments subregion.

1 Introduction

The AdS/CFT correspondence provides a controlled environment to investigate the deep relation between quantum information and gravity. In holography, entanglement entropy is proportional to the area of extremal surfaces [1]. This result provides a more general framework to the idea that the black hole entropy is proportional to the area of the event horizon [2]. The issue of entanglement entropy in AdS/CFT has been studied in recent years by many authors, see [3, 4] for reviews.

The desire of understanding the interior of the black hole horizon motivates the investigation of less traditional quantum information quantities. The growth of the Einstein-Rosen bridge continues for a much longer time scale compared to the thermalization time, where entanglement entropy saturates. This motivates the introduction in holography of the new quantum information concept of computational complexity [5, 6, 7, 8]. Given a set of elementary quantum unitary operations and a reference state, quantum complexity is heuristically defined as the minimal number of elementary operations needed to reach a generic state starting from the reference one. Therefore complexity gives a measure of the difficulty in preparing a given state starting from a simple reference state. A nice geometrical formalism which involves geodesics in the space of unitary evolutions was introduced in [9, 10]. In recent years, several attempts have been done to define complexity in quantum field theory, e.g. [11, 12, 13, 14]. When considering free field theories, it is possible to regularize the theory by placing it on a lattice, which reduces the computation of complexity to the case of a set of harmonic oscillators. It is still challenging to define complexity for interacting field theories. In 2 dimensions, an approach involving the Liouville action was proposed in [15, 16, 17].

A few proposals have been suggested for the holographic dual of complexity:

- complexity=volume (CV) [5, 6, 7] relates complexity to the volume V the extremal surfaces anchored at the boundary

$$\mathcal{C}_V = \text{Max} \left(\frac{V}{GL} \right) , \tag{1.1}$$

  where G is the Newton constant and L the AdS length.

- complexity=action (CA) [18, 19] relates it to the action evaluated on the Wheeler-De Witt (WDW) patch, which is the domain of dependence of the volume extremal surface

$$\mathcal{C}_A = \frac{I_{WDW}}{\pi} . \tag{1.2}$$

- complexity=spacetime volume (CV 2.0) [20] links complexity with the spacetime volume $\hat{V}$ of the WDW patch

$$\mathcal{C}_{V2.0} = \frac{\hat{V}}{GL^2} . \tag{1.3}$$

Holographic complexity has been recently studied by many groups in various asymptotically AdS gravity backgrounds, see for example [21, 22, 23, 24, 25, 26, 27, 28, 29, 30, 31, 32, 33]. The study of holographic complexity can be generalized also to spacetimes with other UV asymptotics, such as Lifshitz theories and Warped AdS black holes, see e.g. [34, 35, 36, 37, 38].

An interesting extension of the holographic complexity conjecture is to consider restrictions to subregions of the boundary conformal field theory. This is physically motivated by analogy with the entanglement entropy. Each of the holographic complexity conjectures has a natural subregion generalization:

- the subregion CV [40] proposes that the complexity associated to a boundary region A is proportional to the volume of the extremal spatial volume bounded by A and by its Hubeny-Rangamani-Takayanagi (HRT) surface [41].

- subregion CA [42] (or CV 2.0) proposes that the subregion complexity is given by the action (or the spacetime volume, respectively) of the intersection between the WDW patch and the entanglement wedge [39].

Subregion complexity has been recently studied by many authors, e.g. [43, 44, 45, 46, 47, 48, 49, 50, 51, 52, 53, 54, 55]. A few options for the quantum information dual of holographic subregion complexity have been proposed, such as purification or basis complexity [46]. In order to identify the correct quantum field theory dual, it is necessary to compute subregion complexity in many physical situations.

In this paper we study the CA and CV 2.0 conjectures for subregions in asymptotically AdS$_3$ spacetime. We find the following analytic result for the subregion complexity of a segment of length l in the BTZ [56, 57] black hole background:

$$\mathcal{C}_A^{\mathrm{BTZ}} = \frac{l}{\varepsilon}\frac{c}{6\pi^2}\log\left(\frac{\tilde{L}}{L}\right) - \log\left(\frac{2\tilde{L}}{L}\right)\frac{S^{\mathrm{BTZ}}}{\pi^2} + \frac{1}{24}c\,, \qquad (1.4)$$

where $\tilde{L}$ is a free scale of the counterterm in the action [21], ε is the UV cutoff, c the CFT central charge and S^{BTZ} the Ryu-Takayanagi (RT) entanglement entropy of the segment subregion. This shows a direct connection at equilibrium, in the case of the one segment subregion, between action complexity and entropy. This expression is also valid for the particular case of AdS$_3$, which was previously studied in [42, 25]. We find a similar expression also for the CV 2.0 conjecture, see eq. (3.30).

One may wonder if such a simple connection between subregion complexity and entanglement entropy is valid also for more general subsystems. For this reason, we compute action complexity in the case of a two segments subregion in AdS$_3$. This quantity has as before a linear divergence proportional to the total size of the region and a log divergence proportional to the divergent part of the entropy. However, if the separation between the two disjoint segments is small, there is no straightforward relation between the finite part of complexity and entropy, see eq. (4.23).

The paper is organised as follows. In section 2 we review the subregion complexity calculation for a segment in AdS$_3$. In section 3 we compute the subregion complexity for a segment in the BTZ background, and we show that it is related to the entanglement entropy. In section 4 we calculate subregion complexity for two disjoint segments in AdS$_3$. In section 5 we discuss mutual complexity. In appendix A we compute the single segment subregion complexity in the BTZ background with a different regularization.

Note added: While we were finalizing the writing of this paper, Ref. [58] appeared on the arXiv. They also suggest a relation between terms in subregion complexity and entanglement entropy. In particular, in their eqs. (7.8) and (7.9), they guess (supported by numerics) some expressions for subregion CA and CV 2.0 for a segment in global AdS$_3$. These expressions should be connected via analytic continuation to our calculations for subregion complexity of a segment in BTZ, eq. (1.4) and (3.30).

2 Subregion complexity for a segment in AdS$_3$

It is useful to review the AdS$_3$ calculation [42, 25, 58] to set up the notation and the procedure, and as a warm-up for the more complicated BTZ case. because afterwards we

will be interested in the more complicated BTZ case. Let us consider gravity with negative cosmological constant in $2 + 1$ dimensions

$$S = \frac{1}{16\pi G} \int \left(R + \frac{2}{L^2} \right) \sqrt{-g} \, d^3x \,, \tag{2.1}$$

which has as a solution AdS$_3$ spacetime, whose metric in Poincaré coordinates reads

$$ds^2 = \frac{L^2}{z^2} \left(-dt^2 + dz^2 + dx^2 \right) \,. \tag{2.2}$$

The AdS curvature is $R = -6/L^2$ and L is the AdS length. The central charge of the dual conformal field theory is:

$$c = \frac{3L}{2G} \,. \tag{2.3}$$

Two common regularizations [42] are used in the CA conjecture (see figure 1):

- Regularization A: the WDW patch is built starting from the boundary $z = 0$ of the spacetime and a cutoff is then introduced at $z = \varepsilon$.

- Regularization B: the WDW patch is built from the surface $z = \varepsilon$.

We will mostly use regularization B; comparison with regularization A is discussed in Appendix A.
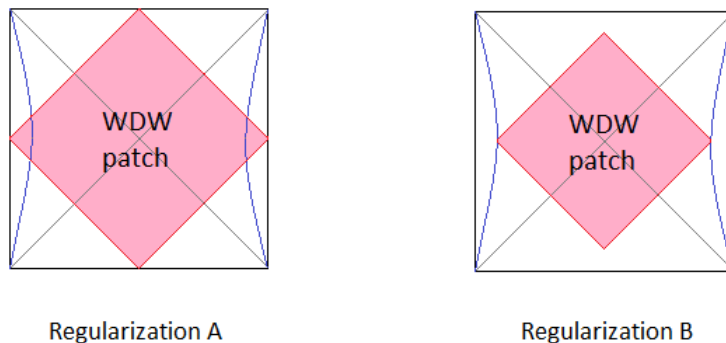

Figure 1: The two regularizations commonly used in the CA conjecture.

We consider a subregion on the boundary given by a strip of length l and for convenience we take $x \in \left[-\frac{l}{2}, \frac{l}{2} \right]$, at the constant time slice $t = 0$. The geometry relevant to the computation of action complexity is the intersection between the entanglement wedge [39] of the subregion with the WDW patch [18, 19], see figure 2. We will consider all the contributions to the action involving null surface and joint terms introduced in [21]. The intersection point between the WDW patch, the entanglement wedge and the boundary at $z = 0$, $x = \pm l/2$ gives a codimension-3 joint, that a priori can contribute. This kind of joint exists just in regularization B; we will check that regularization A gives a similar result in Appendix A. So we believe that this joint at most shifts the action of an overall constant.

We use regularization B with a cutoff a $z = \varepsilon$. The Ryu-Takayanagi (RT) surface [1] is given by the space-like geodesic:

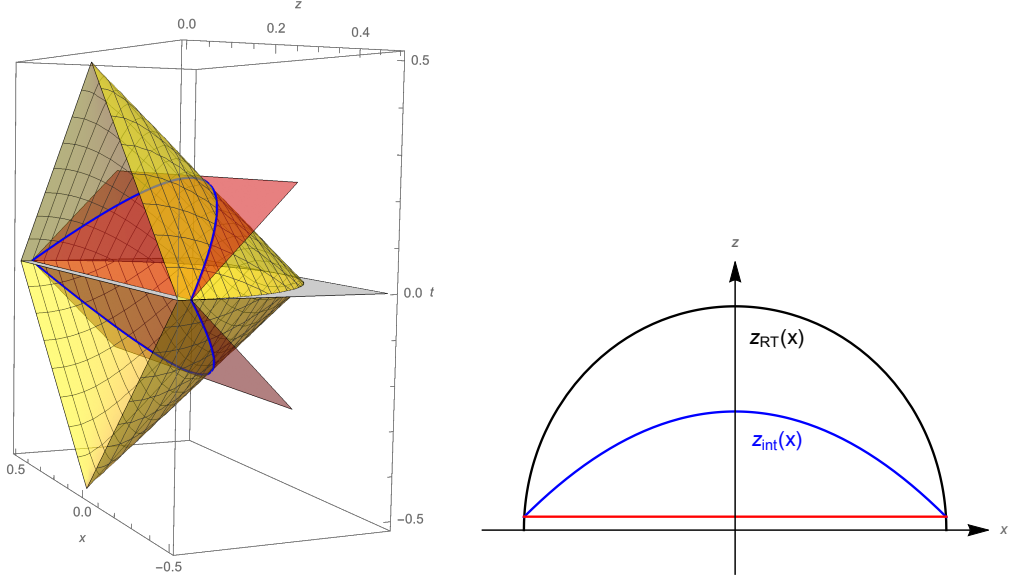$$t = 0 \,, \qquad z^2 + x^2 = \left(\frac{l}{2} \right)^2 \,, \tag{2.4}$$

3

Figure 2: Left: Intersection of WDW patch with entanglement wedge in the (x, z, t) space. The boundary of the entanglement wedge is in yellow, while the boundary of the WDW patch is in red. Right: intersections in the (x, z) plane, with z_{RT} in black, z_{int} in blue and the cutoff $z = \varepsilon$ in red.

which is a circle of radius $l/2$. It is convenient to introduce:

$$z_{RT} = \sqrt{\left(\frac{l}{2}\right)^2 - x^2} \, . \tag{2.5}$$

The entanglement wedge is a cone whose null boundaries are parameterized by

$$t_{\text{EW}} = \pm \left(\frac{l}{2} - \sqrt{z^2 + x^2}\right) \, . \tag{2.6}$$

The boundaries of the WDW patch, which are attached to the regulator surface, are described by the equations

$$t_{\text{WDW}} = \pm (z - \varepsilon) \, . \tag{2.7}$$

The intersection curve between the null boundary of the WDW patch and the one of the entanglement wedge is

$$z_{\text{int}} = \frac{(l + 2\varepsilon)^2 - 4x^2}{4(l + 2\varepsilon)} \qquad \text{or} \qquad x_{\text{int}} = \frac{1}{2}\sqrt{(l + 2\varepsilon)(l - 4z + 2\varepsilon)} \, . \tag{2.8}$$

The UV cutoff ε for the radial coordinate z intersects the RT surface at the following value of x:

$$x_{\text{max}} = \sqrt{\left(\frac{l}{2}\right)^2 - \varepsilon^2} \, . \tag{2.9}$$

This shift from $x = l/2$ is necessary for a correct regularization of the on-shell action. Following [21], the action includes several terms

$$I = I_{\text{bulk}} + I_{\text{b}} + I_{\text{ct}} + I_{\mathcal{J}} \, , \tag{2.10}$$

where I_{bulk} is the bulk term (see eq. 2.1), I_{b} the null boundary term (see (2.15)), I_{ct} the counterterm (2.19) and $I_{\mathcal{J}}$ the null joint contribution (2.22).

4

2.1 Bulk term

The curvature is constant and so the Einstein-Hilbert term (2.1) is proportional to the spacetime volume. We can split the bulk contribution in two parts, based on the intersection between the WDW patch and the entanglement wedge, which we parametrize with the function $z_{int}(x)$. In the first region the WDW patch is subtended by the entanglement wedge. Consequently, we integrate along time $0 \leq t \leq t_{\text{WDW}}(z)$, then the radial direction along $\varepsilon \leq z \leq z_{\text{int}}(x)$, and finally along the coordinate $0 \leq x \leq x_{\max}$:

$$I_{\text{bulk}}^1 = -\frac{L}{4\pi G} \int_0^{x_{max}} dx \int_\varepsilon^{z_{int}} dz \int_0^{t_{WDW}} dt \, \frac{1}{z^3} \tag{2.11}$$

In the second region the entanglement wedge is under the WDW patch, then the integration involves the endpoints $0 \leq t \leq t_{\text{EW}}(z,x), z_{\text{int}}(x) \leq z \leq z_{\text{RT}}(x)$ and finally $0 \leq x \leq x_{\max}$:

$$I_{\text{bulk}}^2 = -\frac{L}{4\pi G} \int_0^{x_{max}} dx \int_{z_{int}}^{z_{RT}} dz \int_0^{t_{EW}} dt \, \frac{1}{z^3} \tag{2.12}$$

A direct evaluation of the integrals gives:

$$\begin{aligned}
I_{\text{bulk}}^1 &= -\frac{L}{16\pi G} \frac{l}{\varepsilon} - \frac{L}{4\pi G} \log\left(\frac{\varepsilon}{l}\right) - \frac{L}{8\pi G} \, . \\
I_{\text{bulk}}^2 &= \frac{L}{8\pi G} \log\left(\frac{\varepsilon}{l}\right) + \frac{L(\pi^2+8)}{64\pi G} \, .
\end{aligned} \tag{2.13}$$

The total result of the bulk action is:

$$I_{\text{bulk}}^{\text{AdS}} = 4(I_{\text{bulk}}^1 + I_{\text{bulk}}^2) = -\frac{L}{4\pi G} \frac{l}{\varepsilon} + \frac{L}{2\pi G} \log\left(\frac{l}{\varepsilon}\right) + \frac{L\pi}{16G} \, . \tag{2.14}$$

2.2 Null boundary counterterms

A hypersurface described by the scalar equation $\Phi(x^a) = 0$ has a normal vector $k_a = -\partial_a \Phi$. If the hypersurface is null, $k_a k^a = 0$ and then it can be shown [59] that the hypersurface is generated by null geodesics, which have k^α as a tangent vector.

In correspondence of a null boundary, the following term should be added to the action [21]:

$$I_b = \int dS \, d\lambda \, \sqrt{\sigma} \kappa \, , \tag{2.15}$$

where λ is the geodesic parameter, S the transverse spatial directions, σ is the determinant of the induced metric on S and κ is defined by the geodesic equation

$$k^\mu D_\mu k^\alpha = \kappa \, k^\alpha \, . \tag{2.16}$$

In our case, the null normals to the WDW patch and the entanglement wedge are given respectively by the following 1-forms:

$$\mathbf{k}^\pm = \alpha \, (\pm dt - dz) \, , \qquad \mathbf{w}^\pm = \beta \left(\pm dt + \frac{zdz}{\sqrt{z^2+x^2}} + \frac{xdx}{\sqrt{z^2+x^2}} \right) \, , \tag{2.17}$$

where α, β are arbitrary constants that will cancel in the final result. We denote by $(k^\pm)^\mu$ and $(w^\pm)^\mu$ the corresponding vectors. It can be checked that they correspond to an affine parametrization of their null surfaces, i.e.

$$(k^\pm)^\mu D_\mu (k^\pm)^\alpha = 0 \, , \qquad (w^\pm)^\mu D_\mu (w^\pm)^\alpha = 0 \, . \tag{2.18}$$

The term (2.15) vanishes in our calculation because we used an affine parameterization, see eq. (2.18).

We still need to include the contribution from the counterterm, which ensures the reparameterization invariance of the action:

$$I_{\text{ct}} = \frac{1}{8\pi G} \int d\lambda \, dS \, \sqrt{\sigma} \, \Theta \, \log \left| \tilde{L} \, \Theta \right| , \tag{2.19}$$

where Θ is the expansion scalar of the boundary geodesics and $\tilde{L}$ is an arbitrary scale. If an affine parameterization is used, we can use the result [59]

$$\Theta = D_\mu k^\mu . \tag{2.20}$$

We can then evaluate eq. (2.19) on each boundary:

- The counterterm on the entanglement wedge boundary vanishes because $\Theta = 0$. This agrees with the calculations in [39].

- For the boundary of the WDW patch we obtain:

$$
\begin{aligned}
I_{\text{ct}}^{\text{WDW}} &= -\frac{L}{2\pi G} \int_0^{x_{\max}} dx \int_\varepsilon^{z_{\text{int}}} \frac{dz}{z^2} \log \left| \alpha \frac{\tilde{L} z}{L^2} \right| \\
&= \frac{L}{4\pi G} \frac{l}{\varepsilon} \left[1 + \log \left(\alpha \frac{\tilde{L}\varepsilon}{L^2} \right) \right] + \frac{L}{4\pi G} \log \left(\frac{\varepsilon}{l} \right) \log \left(\alpha^2 \frac{\varepsilon l \tilde{L}^2}{L^4} \right) \\
&+ \frac{L}{2\pi G} \log \left(\frac{\varepsilon}{l} \right) + \frac{L\pi}{12G} .
\end{aligned}
\tag{2.21}
$$

2.3 Joint terms

The contribution to the gravitational action coming from a codimension-2 joint, given by intersection of two codimension-1 null surfaces [21], is

$$I_{\mathcal{J}} = \frac{\eta}{8\pi G} \int_{-x_{max}}^{x_{max}} dx \sqrt{\sigma} \log \left| \frac{\mathbf{a_1} \cdot \mathbf{a_2}}{2} \right| \tag{2.22}$$

where σ is the induced metric determinant on the codimension-2 surface, $\mathbf{a_1}$ and $\mathbf{a_2}$ are the null normals to the two intersecting codimension-1 null surfaces and $\eta = \pm 1$. The overall sign η can be determined as follows: if the outward direction from a given null surface points to the future, we should assign $\eta = 1$ if the joint is at the future of the null surface, and $\eta = -1$ if it is at the past. If the outward direction from a given null surface points to the past, $\eta = -1$ if the joint is at the future, and $\eta = 1$ if it is at the past.

The four joints give the following contributions:

- The first joint is at the cutoff $z = \varepsilon$; we find

$$\sqrt{\sigma} = \frac{L}{\varepsilon}, \qquad \log \left| \frac{\mathbf{k}^- \cdot \mathbf{k}^+}{2} \right| = \log \left| \alpha^2 \frac{\varepsilon^2}{L^2} \right| , \tag{2.23}$$

and then from the general expression (2.22)

$$I_{\mathcal{J}}^{\text{cutoff}} = -\frac{L}{4\pi G} \frac{l}{\varepsilon} \log \left(\alpha \frac{\varepsilon}{L} \right) . \tag{2.24}$$

- The second joint to compute involves the RT surface:

$$\sqrt{\sigma} = \frac{2lL}{l^2 - 4x^2}\,, \qquad \log\left|\frac{\mathbf{w}^+ \cdot \mathbf{w}^-}{2}\right| = \log\left|\beta^2\frac{l^2 - 4x^2}{4L^2}\right|\,, \tag{2.25}$$

which gives

$$I_{\mathcal{J}}^{\mathrm{RT}} = \frac{L}{4\pi G}\log\left(\frac{\varepsilon}{l}\right)\log\left(\frac{\beta^2\varepsilon l}{L^2}\right) + \frac{L\pi}{48G}\,. \tag{2.26}$$

- The last joint terms come from the intersections between the null boundaries of the WDW patch and the ones of the entanglement wedge:

$$\sqrt{\sigma} = \frac{4L(l + 2\varepsilon)}{(l - 2x + 2\varepsilon)(l + 2x + 2\varepsilon)}\,, \tag{2.27}$$

$$\log\left|\frac{\mathbf{k}^+ \cdot \mathbf{w}^+}{2}\right| = \log\left|\frac{(l - 2x + 2\varepsilon)(l + 2x + 2\varepsilon)}{4L(4x^2 + (l + 2\varepsilon)^2)}\right|^2\,. \tag{2.28}$$

Therefore the joints evaluate to

$$I_{\mathcal{J}}^{\mathrm{int}} = -\frac{L}{2\pi G}\log\left(\frac{\varepsilon}{l}\right)\log\left(\frac{\alpha\beta}{2}\frac{\varepsilon l}{L^2}\right) - \frac{5\pi L}{48G}\,. \tag{2.29}$$

Summing all the joint contributions we find

$$I_{\mathcal{J}}^{\mathrm{tot}} = -\frac{L}{4\pi G}\frac{l}{\varepsilon}\log\left(\alpha\frac{\varepsilon}{L}\right) + \frac{L}{4\pi G}\log\left(\frac{\varepsilon}{l}\right)\log\left(\frac{4L^2}{\alpha^2\varepsilon l}\right) - \frac{\pi L}{12G}\,. \tag{2.30}$$

Note that the dependence on the normalization constant β of the normals cancels in (2.30); this is due to the fact that the null surfaces which have the RT surface as boundaries have vanishing expansion parameter Θ. Also, when summing the joint term (2.30) with the counterterm contribution (2.21) the double log terms cancel and the dependence on α cancels.

2.4 Complexities

Summing all the contributions, the action complexity is:

$$\mathcal{C}_A^{\mathrm{AdS}} = \frac{I_{\mathrm{tot}}^{\mathrm{AdS}}}{\pi} = \frac{c}{3\pi^2}\left\{\frac{l}{2\varepsilon}\log\left(\frac{\tilde{L}}{L}\right) - \log\left(\frac{2\tilde{L}}{L}\right)\log\left(\frac{l}{\varepsilon}\right) + \frac{\pi^2}{8}\right\}\,. \tag{2.31}$$

Instead, from eq. (2.14), the spacetime volume complexity is:

$$\mathcal{C}_{V2.0}^{\mathrm{AdS}} = \frac{2}{3}c\left\{\frac{l}{\varepsilon} - 2\log\left(\frac{l}{\varepsilon}\right) - \frac{\pi^2}{4}\right\}\,. \tag{2.32}$$

Both the calculations are in agreement with [58]. In both the expressions for the complexity we recognize a term proportional to the entanglement entropy of the segment:

$$S^{\mathrm{AdS}} = \frac{c}{3}\log\left(\frac{l}{\varepsilon}\right)\,. \tag{2.33}$$

This suggests that the complexity for a single interval has a leading divergence proportional to the length of the subregion on the boundary, a subleading divergence proportional to the entanglement entropy and a constant finite piece. We test this expression for the BTZ case in the next section.

3 Subregion complexity for a segment in the BTZ black hole

We consider the metric of the planar BTZ black hole in $2+1$ dimensions with non-compact coordinates (t, z, x)

$$ds^2 = \frac{L^2}{z^2}\left(-f dt^2 + \frac{dz^2}{f} + dx^2\right), \qquad f = 1 - \left(\frac{z}{z_h}\right)^2, \tag{3.1}$$

where L is the AdS radius and z_h is the position of the horizon. The mass, the temperature and the entropy are:

$$M = \frac{L^2}{8Gz_h^2}, \qquad T = \frac{1}{2\pi z_h}, \qquad S = \frac{\pi L^2}{2Gz_h}. \tag{3.2}$$

The geometry needed to evaluate the subregion complexity for a segment is shown in figure 3
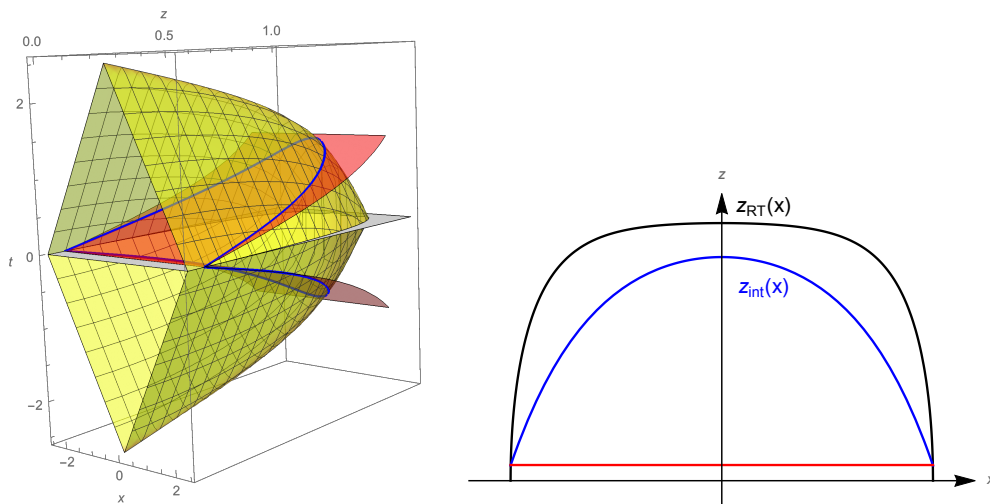

Figure 3: Region relevant to the action computation for a segment in the BTZ case, for $l = 5$. Left: Intersection of WDW patch with entanglement wedge in the (x, z, t) space. The boundary of the entanglement wedge is in yellow, while the boundary of the WDW patch is in red. Right: intersections in the (x, z) plane, with z_{RT} in black, z_{int} in blue and the cutoff $z = \varepsilon$ in red.

The RT surface is a spacelike geodesic which lies on a constant time slice $t = 0$ and which is anchored at the edges of the boundary subregion [63]:

$$x_{\pm}(z) = \frac{1}{4}z_h \left[\log\left(\frac{J+1}{J-1}\right)^2 + \log\left(\frac{z_h^2 - Jz^2 \pm \sqrt{z_h^4 - (1+J^2)z_h^2 z^2 + J^2 z^4}}{z_h^2 + Jz^2 \pm \sqrt{z_h^4 - (1+J^2)z_h^2 z^2 + J^2 z^4}}\right)^2\right], \tag{3.3}$$

where

$$J = \coth\left(\frac{l}{2z_h}\right). \tag{3.4}$$

The turning point of the geodesic is at $x_{\pm}(z_*) = 0$, where

$$z_* = z_h \tanh\left(\frac{l}{2z_h}\right). \tag{3.5}$$

8

Since $z_* < z_h$ for every value of the boundary subregion size l, the geodesic never penetrates inside the event horizon of the black hole. It is convenient to invert eq. (3.3):

$$z_{RT} = z_h \sqrt{\frac{\cosh\left(\frac{l}{z_h}\right) - \cosh\left(\frac{2x}{z_h}\right)}{\cosh\left(\frac{l}{z_h}\right) + 1}}.$$

(3.6)

In our static case, the entanglement wedge coincides with the causal wedge [60, 61, 62], which can be constructed by sending null geodesics from the causal diamond on the boundary into the bulk. The explicit expressions of such geodesics are [61]

$$
\begin{aligned}
\tilde{x}_{\text{EW}}(z, j) &= \frac{z_h}{2} \log\left(\frac{\sqrt{z_h^2 + j^2(z^2 - z_h^2)} + jz}{\sqrt{z_h^2 + j^2(z^2 - z_h^2)} - jz}\right), \\
\tilde{t}_{\text{EW}}(z, j) &= \pm\left[\frac{l}{2} + \frac{z_h}{2} \log\left(\frac{\sqrt{z_h^2 + j^2(z^2 - z_h^2)} - z}{\sqrt{z_h^2 + j^2(z^2 - z_h^2)} + z}\right)\right].
\end{aligned}
$$

(3.7)

We obtain an analytical expression for the boundary of the entanglement wedge in terms of a unique explicit relation between (t, z, x) by determining $j = j(z, x)$ from the first equation in (3.7) and then inserting it into the second equation of (3.7). The result can be written as

$$t_{\text{EW}} = \pm\left[\frac{l}{2} - z_h \operatorname{arccoth}\left(\frac{\sqrt{2} z_h \cosh\left(\frac{x}{z_h}\right)}{\sqrt{2z^2 + z_h^2 \cosh\left(\frac{2x}{z_h}\right) - z_h^2}}\right)\right].$$

(3.8)

The WDW patch is delimited by the radial null geodesics:

$$t_{\text{WDW}} = \pm\frac{z_h}{4} \log\left(\frac{z_h + z}{z_h - z}\frac{z_h - \varepsilon}{z_h + \varepsilon}\right)^2.$$

(3.9)

The intersection between the boundary of the WDW patch and the entanglement wedge is:

$$t_{\text{int}} = t_{\text{WDW}}, \qquad z_{\text{int}} = z_h \frac{\cosh\left[\frac{l}{2z_h} + \operatorname{arctanh}\left(\frac{\varepsilon}{z_h}\right)\right] - \cosh\left(\frac{x}{z_h}\right)}{\sinh\left[\frac{l}{2z_h} + \operatorname{arctanh}\left(\frac{\varepsilon}{z_h}\right)\right]}.$$

(3.10)

We plot this curve in Fig. 3.

As in the AdS case, we denote by $x_{\max}$ the maximum value of the transverse coordinate, which is reached when we evaluate the RT surface at $z = \varepsilon$:

$$x_{\max} = z_h \operatorname{arccosh}\left[\sqrt{1 - \frac{\varepsilon^2}{z_h^2}} \cosh\left(\frac{l}{2z_h}\right)\right].$$

(3.11)

3.1 Bulk contribution

We split the integration region as in the AdS case, see eqs. (2.11, 2.12). The total bulk action then is $I_{\text{bulk}} = 4(I_{\text{bulk}}^1 + I_{\text{bulk}}^2)$. A direct calculation gives:

$$
\begin{aligned}
I_{\text{bulk}} = \frac{L}{8\pi G z_h} \int_0^{x_{max}(\varepsilon)} dx &\left\{ \frac{4\sinh\left[\frac{l}{2z_h} + \operatorname{arctanh}\left(\frac{\varepsilon}{z_h}\right)\right]}{\cosh\left(\frac{l}{2z_h} + \operatorname{arctanh}\left(\frac{\varepsilon}{z_h}\right)\right) - \cosh\left(\frac{x}{z_h}\right)} - \frac{4z_h}{\varepsilon} \right. \\
&\left. + 2\coth\left(\frac{x}{z_h}\right) \log\left|\frac{\sinh\left(\frac{l-2x}{2z_h}\right) \sinh^2\left[\frac{l+2x+2z_h \operatorname{arctanh}(\varepsilon/z_h)}{4z_h}\right]}{\sinh\left(\frac{l+2x}{2z_h}\right) \sinh^2\left[\frac{l-2x+2z_h \operatorname{arctanh}(\varepsilon/z_h)}{4z_h}\right]}\right| \right\}.
\end{aligned}
$$

(3.12)

9

This integral can be computed analytically, and gives the CV 2.0 complexity in eq (3.30).

3.2 Null normals

In order to compute the counterterms due to the null surfaces and the joint contributions, the null normals are needed. It is convenient to use an affine parameterization, which can be found using the following Lagrangian description of geodesics:

$$\mathcal{L} = \frac{L^2}{z^2} \left(-f(z)\, \dot{t}^2 + \frac{\dot{z}^2}{f(z)} + \dot{x}^2 \right) \tag{3.13}$$

where the dot represents the derivative with respect to the affine parameter λ. Since the Lagrangian does not depend on t and x, we have two constants of motion

$$E = -\frac{1}{2}\frac{\partial \mathcal{L}}{\partial \dot{t}} = \frac{L^2}{z^2} f(z)\, \dot{t} \,, \qquad J = \frac{1}{2}\frac{\partial \mathcal{L}}{\partial \dot{x}} = \frac{L^2}{z^2}\, \dot{x} \,. \tag{3.14}$$

Imposing the null condition $\mathcal{L} = 0$ and making use of eq. (3.14) leads to

$$\dot{z} = \pm \frac{z^2}{L^2}\, \sqrt{E^2 - J^2 f(z)} \,. \tag{3.15}$$

Therefore, from eqs. (3.14) and (3.15), the tangent vector to the null geodesic is

$$V^\mu = \left(\dot{t},\, \dot{z},\, \dot{x} \right) = \left(\frac{z^2}{L^2 f(z)} E,\, \pm \frac{z^2}{L^2}\, \sqrt{E^2 - J^2 f(z)},\, \frac{z^2}{L^2} J \right) \,. \tag{3.16}$$

Lowering the contravariant index with the metric tensor, we get the normal 1-form to the null geodesic

$$\mathbf{V} = V_\mu dx^\mu = -E\, dt \pm \frac{\sqrt{E^2 - J^2 f(z)}}{f(z)}\, dz + J\, dx \,. \tag{3.17}$$

The null geodesics which bound the WDW patch are x-constant curves, and so $J = 0$. This gives the following normals:

$$\mathbf{k}^+ = k_\mu^+ dx^\mu = \alpha \left(dt - \frac{dz}{f(z)} \right) \,, \qquad \mathbf{k}^- = k_\mu^- dx^\mu = \alpha \left(-dt - \frac{dz}{f(z)} \right) \,, \tag{3.18}$$

where α is an arbitrary constant.

The null geodesics that bound the entanglement wedge are normal to the RT surface, i.e.

$$V_\mu \frac{dX_{RT}^\mu(x)}{dx} = 0 \,, \qquad X_{\mathrm{RT}}^\mu(x) = (0, z_{RT},\, x) \,, \tag{3.19}$$

where z_{RT} is given in eq. (3.6). With this condition and eqs. (3.17) and (3.19), we find a relation between the two constants of motion E and J which then gives (for $t > 0$ and $t < 0$ respectively)

$$\mathbf{w}^\pm = w_\mu^\pm dx^\mu = \beta \left(\pm dt + a\, dz + b\, dx \right) \,, \tag{3.20}$$

where

$$a = \frac{e^{-\frac{x}{z_h}} \left(e^{\frac{2x}{z_h}} + 1 \right) z z_h^2}{\left(z_h^2 - z^2 \right) \sqrt{4z^2 + e^{-\frac{2x}{z_h}} \left(e^{\frac{2x}{z_h}} - 1 \right)^2 z_h^2}} \,, \qquad b = \frac{e^{-\frac{x}{z_h}} \left(e^{\frac{2x}{z_h}} - 1 \right) z_h}{\sqrt{4z^2 + e^{-\frac{2x}{z_h}} \left(e^{\frac{2x}{z_h}} - 1 \right)^2 z_h^2}} \,. \tag{3.21}$$

3.3 Null boundaries and counterterms

The term in eq. (2.15) vanishes because we used an affine parameterization. The counterterm in eq. (2.19) gives:

- For the null normals of the boundary of the entanglement wedge, this contribution vanishes because $\Theta = D_\mu (w^\pm)^\mu = 0$.

- For the null normals of the boundary of the WDW patch, a direct calculation gives $\Theta = \frac{\alpha z}{L^2}$ and:

$$
I_{\text{ct}}^{\text{WDW}} = -\frac{L}{2\pi G} \int_0^{x_{\max}} dx \int_\varepsilon^{z_{\text{int}}(x)} dz \, \frac{1}{z^2} \log \left| \frac{\tilde{L}}{L^2} \, \alpha z \right| =
$$

$$
= \frac{L}{2\pi G} \int_0^{x_{\max}} dx \left\{ \frac{1 + \log \left| \frac{\tilde{L}}{L^2} \, \alpha\varepsilon \right|}{\varepsilon} + \frac{\sinh \left(\frac{l}{2z_h} + \operatorname{arctanh} \left(\frac{\varepsilon}{z_h} \right) \right)}{z_h \left[\cosh \left(\frac{x}{z_h} \right) - \cosh \left(\frac{l}{2z_h} \right) + \operatorname{arctanh} \left(\frac{\varepsilon}{z_h} \right) \right]} \times \right.
$$

$$
\left. \times \left(1 + \log \left| \frac{\tilde{L} z_h \alpha}{L^2} \frac{\cosh \left(\frac{l}{2z_h} + \operatorname{arctanh} \left(\frac{\varepsilon}{z_h} \right) \right) - \cosh \left(\frac{x}{z_h} \right)}{\cosh \left(\frac{l}{2z_h} + \operatorname{arctanh} \left(\frac{\varepsilon}{z_h} \right) \right)} \right| \right) \right\} .
$$

(3.22)

3.4 Joint contributions

We evaluate the joint terms in eq (2.22):

- The joint at the cutoff gives:

$$
I_{\mathcal{J}}^{\text{cutoff}} = -\frac{L}{4\pi G} \int_0^{x_{\max}} \frac{dx}{\varepsilon} \left| \frac{\alpha^2 z_h^2 \varepsilon^2}{L^2 (z_h^2 - \varepsilon^2)} \right| .
$$

(3.23)

- The joint at the RT surface:

$$
I_{\mathcal{J}}^{\text{RT}} = -\frac{L}{4\pi G z_h} \int_0^{x_{\max}} dx \, \frac{\sinh \left(\frac{l}{z_h} \right)}{\cosh \left(\frac{l}{z_h} \right) - \cosh \left(\frac{2x}{z_h} \right)} \log \left| \frac{\beta^2 z_h^2}{2L^2} \frac{\cosh \left(\frac{l}{z_h} \right) - \cosh \left(\frac{2x}{z_h} \right)}{\cosh^2 \left(\frac{x}{z_h} \right)} \right| .
$$

(3.24)

- The joints coming from the intersection between the null boundaries of the WDW patch and the ones of the entanglement wedge give:

$$
I_{\mathcal{J}}^{\text{int}} = \frac{L}{2\pi G z_h} \int_0^{x_{\max}} dx \, \frac{\sinh \left(\frac{l}{2z_h} + \operatorname{arctanh} \left(\frac{\varepsilon}{z_h} \right) \right)}{\cosh \left(\frac{l}{2z_h} + \operatorname{arctanh} \left(\frac{\varepsilon}{z_h} \right) \right) - \cosh \left(\frac{x}{z_h} \right)} \times
$$

$$
\times \log \left| \frac{e^{x/z_h} \alpha \beta z_h^2}{L^2} \frac{\left[\cosh \left(\frac{l}{2z_h} + \operatorname{arctanh} \left(\frac{\varepsilon}{z_h} \right) \right) - \cosh \left(\frac{x}{z_h} \right) \right]^2}{1 + e^{2x/z_h} \cosh \left(\frac{l}{2z_h} + \operatorname{arctanh} \left(\frac{\varepsilon}{z_h} \right) \right) - 2 e^{x/z_h}} \right| .
$$

(3.25)

All the joints contributions and the counterterm are regularized by the cutoff ε.

3.5 Complexities

We performed all the integrals analytically and we further simplified the result using various dilogarithm identities, including the relation:

$$8\,\text{Re}\left[\text{Li}_2\left(\frac{1+ie^{\frac{y}{2}}}{1+e^{\frac{y}{2}}}\right) - \text{Li}_2\left(\frac{1}{1+e^{\frac{y}{2}}}\right) - \text{Li}_2\left(1+ie^{\frac{y}{2}}\right) - \text{Li}_2\left(\frac{e^{\frac{y}{2}}-i}{1+e^{\frac{y}{2}}}\right)\right] =$$

$$= -\frac{7\pi^2}{6} + 4\left(\log\left(1+e^{\frac{y}{2}}\right)\right)^2 + \log 2\left[2y - 4\log\left(\frac{e^y-1}{y}\right) + 4\log\left(\frac{2}{y}\sinh\frac{y}{2}\right)\right], \quad (3.26)$$

which can be proved by taking a derivative of both side of the equation with respect to y.

The action subregion complexity then is:

$$\mathcal{C}_A^{\text{BTZ}} = \frac{c}{3\pi^2}\left\{\frac{l}{2\varepsilon}\log\left(\frac{\tilde{L}}{L}\right) - \log\left(\frac{2\tilde{L}}{L}\right)\log\left(\frac{2z_h}{\varepsilon}\sinh\left(\frac{l}{2z_h}\right)\right) + \frac{\pi^2}{8}\right\}. \quad (3.27)$$

Introducing the entanglement entropy of an interval

$$S^{\text{BTZ}} = \frac{c}{3}\log\left(\frac{2z_h}{\varepsilon}\sinh\left(\frac{l}{2z_h}\right)\right), \quad (3.28)$$

we can then write it in this form

$$\mathcal{C}_A^{\text{BTZ}} = \frac{l}{\varepsilon}\frac{c}{6\pi^2}\log\left(\frac{\tilde{L}}{L}\right) - \log\left(\frac{2\tilde{L}}{L}\right)\frac{S^{\text{BTZ}}}{\pi^2} + \frac{1}{24}c. \quad (3.29)$$

By integration of (3.12), the subregion spacetime complexity is

$$\mathcal{C}_{V2.0}^{\text{BTZ}} = \frac{2c}{3}\frac{l}{\varepsilon} - 4S^{\text{BTZ}} - \frac{\pi^2}{6}c. \quad (3.30)$$

The divergencies of eqs. (3.29) and (3.30) are the same as in the AdS case eqs. (2.31) and (2.32), which is recovered for $z_h = 0$.

A useful cross-check can be done in the $l \gg z_h$ limit. Keeping just the terms linear in l in eq. (3.27), we find agreement with the subregion complexity $\mathcal{C}_A^{\text{BTZ,R}}$ computed for one side of the Kruskal diagram, see [46, 47]:

$$\mathcal{C}_A^{\text{BTZ,R}} = \frac{c}{6}\frac{l}{\pi^2}\left[\frac{1}{\varepsilon}\log\left(\frac{\tilde{L}}{L}\right) - \frac{1}{z_h}\log\left(\frac{2\tilde{L}}{L}\right)\right]. \quad (3.31)$$

Note that in this limit the $\log\varepsilon$ divergence disappears because it is suppressed by the segment length l.

For comparison, the volume complexity of an interval for the BTZ [40, 44] is:

$$\mathcal{C}_V^{\text{BTZ}} = \frac{2\,c}{3}\left(\frac{l}{\varepsilon} - \pi\right), \quad (3.32)$$

and it is non-trivially independent on temperature. Subregion $\mathcal{C}_V$ at equilibrium is a topologically protected quantity: for multiple intervals, the authors of [44] found the following result using the the Gauss-Bonnet theorem

$$\mathcal{C}_V^{\text{AdS}} = \mathcal{C}_V^{\text{BTZ}} = \frac{2\,c}{3}\left(\frac{l_{tot}}{\varepsilon} + \kappa\right), \quad (3.33)$$
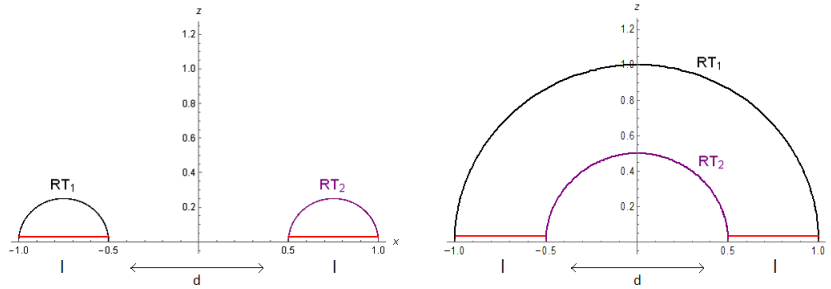
Figure 4: The possible RT surfaces for disjoint subregions of length $l = 0.5$ with a separation $d = 1$, on the slice $t = 0$.

where l_{tot} is the total length of all the segments and κ is the finite part, that depends on topology

$$\kappa = -2\pi\chi + \frac{\pi}{2}\,m\,, \tag{3.34}$$

where χ is the Euler characteristic of the extremal surface (which is equal to 1 for a disk) and m is the number of ninety degrees junctions between RT surface and boundary segments. It would be interesting to see if a similar result could be established for the CA and CV 2.0 conjecture. This motivates us to study the two segment case in the next section.

4 Subregion complexity for two segments in AdS$_3$

In this section we evaluate the holographic subregion action complexity for a disjoint subregion on the AdS_3 spacetime's boundary. We consider two segments of size l with a separation equal to d, located at the spacetime's boundary on the constant time slice $t = 0$. For simplicity, we work with a symmetric configuration, in which the two boundary subregions are respectively given by $x \in [-l - d/2, -d/2]$ and $x \in [d/2, l + d/2]$. According to the values of the subregions size l and of the separation d, there are two possible extremal surfaces anchored at the boundary at the edges of the two subregions [3, 4]:

- The extremal surface (which in this number of dimension is a geodesic) is given by the union of the RT surfaces for the individual subregions. This is the minimal surface for $d > d_0$, where d_0 is a critical distance.

- The extremal surface connects the two subregions. This configuration is minimal for $d < d_0$.

The two cases are shown in Fig. 4. The geodesic with the minimal area provides the holographic entanglement entropy for the union of the disjoint subregions. The critical distance corresponds to the distance for which both the extremal surfaces have the same length, i.e.

$$d_0 = (\sqrt{2} - 1)l\,. \tag{4.1}$$

In the first configuration (see left in Fig. 4), we have two non-intersecting entanglement wedges and so

$$\mathcal{C}_A^1 = 2\,\mathcal{C}_A^{\text{AdS}}\,, \qquad \mathcal{C}_{V2.0}^1 = 2\,\mathcal{C}_{V2.0}^{\text{AdS}}\,. \tag{4.2}$$

For the second configuration (right in Fig. 4), we must perform a new computation. The spacetime region of interest is symmetric both with respect to the $x = 0$ slice and to the $t = 0$ one. As a consequence, we can evaluate the action on the region with $t > 0$ and

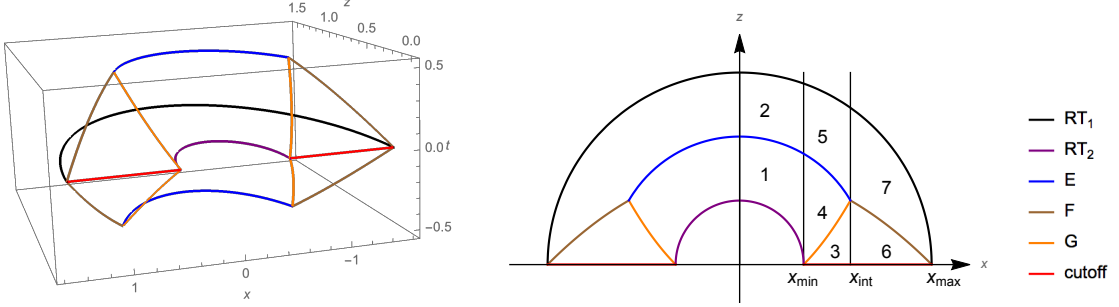$x > 0$ and introduce opportune symmetry factors. A schematic representation is shown in figure 5.

Figure 5: Left: Bulk region relevant to the action subregion calculation for two segments in AdS. Right: projection in the (x, z) plane. The regions in which the bulk integral is splitted are numbered.

The RT surface is the union of the spacelike geodesics anchored at the edges of the region $x \in [-l - d/2, l + d/2]$ and $x \in [-d/2, d/2]$. We will denote such geodesics as RT_1 and RT_2 respectively:

$$z_{RT_1}(x) = \sqrt{\left(\frac{2l + d}{2}\right)^2 - x^2}, \qquad z_{RT_2}(x) = \sqrt{\left(\frac{d}{2}\right)^2 - x^2}. \qquad (4.3)$$

With the introduction of the cutoff surface at $z = \varepsilon$, RT_2 is truncated at $x = x_{min}$ and RT_1 at $x = x_{max}$, defined by

$$x_{min} = \sqrt{\left(\frac{d}{2}\right)^2 - \varepsilon^2}, \qquad x_{max} = \sqrt{\left(\frac{d + 2l}{2}\right)^2 - \varepsilon^2}. \qquad (4.4)$$

The null boundaries of the entanglement wedge can be built by sending null geodesics from RT_1 and RT_2:

$$t_{EW_1} = \frac{2l + d}{2} - \sqrt{z^2 + x^2}, \qquad t_{EW_2} = -\frac{d}{2} + \sqrt{z^2 + x^2}. \qquad (4.5)$$

The WDW patch, anchored at the cutoff in the present regularization, is bounded by the null surface

$$t_{WDW} = z - \varepsilon. \qquad (4.6)$$

The intersection curve E between the null boundaries of the entanglement wedge, (built from RT_1 and RT_2, see eq. (4.5)) is

$$t_E = \frac{l}{2}, \qquad z_E = \frac{1}{2}\sqrt{(d + l)^2 - 4x^2}. \qquad (4.7)$$

The intersection F between the boundary of the WDW patch eq. (4.6) and the null surface anchored at RT_1 is:

$$t_F = \frac{1}{4}\left[d + 2(l - \varepsilon) - \frac{4x^2}{d + 2(l + \varepsilon)}\right], \qquad z_F = t_F + \varepsilon. \qquad (4.8)$$

The intersection G between the WDW patch eq. (4.6) and the null surface anchored at RT_2 gives

$$t_G = -\frac{d}{4} + \frac{x^2}{d - 2\varepsilon} - \frac{\varepsilon}{2}, \qquad z_G = t_G + \varepsilon. \qquad (4.9)$$

14

The intersection among the three curves described above (obtained solving the condition $z_E = z_F = z_G$) gives

$$x_{int}(\varepsilon) = \frac{\sqrt{(d - 2\varepsilon)\left[d + 2\left(l + \varepsilon\right)\right]}}{2} \,. \tag{4.10}$$

4.1 Bulk contribution

As shown in Fig. 5, the total bulk contribution can be divided into 7 parts for computational reasons:

$$I_{bulk} = 4 \sum_{i=1}^{7} I_{bulk}^i \,, \tag{4.11}$$

where

$$
\begin{aligned}
I_{bulk}^1 &= -\frac{L}{4\pi G} \int_0^{x_{min}} dx \int_{z_{RT_2}}^{z_E} dz \int_0^{t_{EW_2}} \frac{dt}{z^3} \\
I_{bulk}^2 &= -\frac{L}{4\pi G} \int_0^{x_{min}} dx \int_{z_E}^{z_{RT_1}} dz \int_0^{t_{EW_1}} \frac{dt}{z^3} \\
I_{bulk}^3 &= -\frac{L}{4\pi G} \int_{x_{min}}^{x_{int}} dx \int_\varepsilon^{z_G} dz \int_0^{t_{WDW}} \frac{dt}{z^3} \\
I_{bulk}^4 &= -\frac{L}{4\pi G} \int_{x_{min}}^{x_{int}} dx \int_{z_G}^{z_E} dz \int_0^{t_{EW_2}} \frac{dt}{z^3} \\
I_{bulk}^5 &= -\frac{L}{4\pi G} \int_{x_{min}}^{x_{int}} dx \int_{z_E}^{z_{RT_1}} dz \int_0^{t_{EW_1}} \frac{dt}{z^3} \\
I_{bulk}^6 &= -\frac{L}{4\pi G} \int_{x_{int}}^{x_{max}} dx \int_\varepsilon^{z_F} dz \int_0^{t_{WDW}} \frac{dt}{z^3} \\
I_{bulk}^7 &= -\frac{L}{4\pi G} \int_{x_{int}}^{x_{max}} dx \int_{z_F}^{z_{RT_1}} dz \int_0^{t_{EW_1}} \frac{dt}{z^3} \,.
\end{aligned}
\tag{4.12}
$$

All the integrals can be evaluated analytically. Since the expressions are rather cumbersome, we will write just the total expression of $\mathcal{C}_{V2.0}^2$ in (4.24).

4.2 Counterterms

The counterterms for the null boundaries of the entanglement wedge vanish as usual. We can separate the counterterm for the null boundaries of the WDW patch in two contributions:

$$
\begin{aligned}
I_{ct,I} &= \frac{L}{2\pi G} \int_{x_{min}}^{x_{int}} dx \int_\varepsilon^{z_G} \frac{dz}{z^2} \log\left(\frac{\tilde{L}\,\alpha\,z}{L^2}\right) , \\
I_{ct,II} &= \frac{L}{2\pi G} \int_{x_{int}}^{x_{max}} dx \int_\varepsilon^{z_F} \frac{dz}{z^2} \log\left(\frac{\tilde{L}\,\alpha\,z}{L^2}\right) .
\end{aligned}
\tag{4.13}
$$

4.3 Joint contributions

We have to include several joint contributions to the action:

- Joints on the cutoff at $z = \varepsilon$. The null normals are

$$\mathbf{k}^\pm = \alpha\left(\pm dt - dz\right) , \tag{4.14}$$

and the contribution is:

$$I_\varepsilon = -\frac{L}{4\pi G} \int_{x_{min}}^{x_{max}} dx \, \frac{\log\left(\frac{\alpha^2 \varepsilon^2}{L^2}\right)}{\varepsilon} = -\frac{L}{2\pi G} \frac{l \, \log\left(\frac{\alpha \varepsilon}{L}\right)}{\varepsilon} \, . \tag{4.15}$$

- Joint on RT_1. The null normals to such surfaces are

$$\mathbf{w_1^\pm} = \beta \left(\pm dt + \frac{z}{\sqrt{z^2 + x^2}} dz + \frac{x}{\sqrt{z^2 + x^2}} dx \right) , \tag{4.16}$$

which gives

$$\begin{aligned} I_{RT_1} &= -\frac{L}{2\pi G} \int_0^{x_{max}} dx \, \frac{d + 2l}{(d + 2l)^2 - 4x^2} \log \frac{\beta^2 \left[(d + 2l)^2 - 4x^2\right]}{4L^2} = \\ &= \frac{L}{4\pi G} \log(\varepsilon) \log\left(\frac{\beta^2 \varepsilon}{L^2}\right) - \frac{L}{4\pi G} \log(d + 2l) \log \frac{(d + 2l)\beta^2}{L^2} + \frac{L\pi}{48G} \, . \end{aligned} \tag{4.17}$$

- Joint on RT_2. The null normals to these surfaces are

$$\mathbf{w_2^\pm} = \gamma \left(\pm dt - \frac{z}{\sqrt{z^2 + x^2}} dz - \frac{x}{\sqrt{z^2 + x^2}} dx \right) , \tag{4.18}$$

and the action is:

$$\begin{aligned} I_{RT_2} &= -\frac{L}{2\pi G} \int_0^{x_{min}} dx \, \frac{d}{d^2 - 4x^2} \log \frac{\gamma^2 \left(d^2 - 4x^2\right)}{4L^2} = \\ &= \frac{L}{4\pi G} \log(\varepsilon) \log\left(\frac{\gamma^2 \varepsilon}{L^2}\right) - \frac{L}{4\pi G} \log(d) \log \frac{d \gamma^2}{L^2} + \frac{L\pi}{48G} \, . \end{aligned} \tag{4.19}$$

- Joints between the two null boundaries of the entanglement wedge, curve E. The normals are $\mathbf{w_1^+}$ and $\mathbf{w_2^+}$. The contribution gives

$$I_E = \frac{L}{\pi G} \int_0^{x_{int}} dx \, \frac{d + l}{(d + l)^2 - 4x^2} \log \left[\frac{\beta \gamma \left[(d + l)^2 - 4x^2\right]}{4L^2} \right] . \tag{4.20}$$

- Joint between the null boundary of the WDW patch and the null boundary of the entanglement wedge anchored at RT_1, curve F. The normals are $\mathbf{k^+}$ and $\mathbf{w_1^+}$. The term gives

$$I_F = \frac{2L}{\pi G} \int_{x_{int}}^{x_{max}} dx \, \frac{d + 2\,(l + \varepsilon)}{(d + 2\,(l + \varepsilon))^2 - 4x^2} \log \left[\frac{\alpha \beta \left[(d + 2\,(l + \varepsilon))^2 - 4x^2\right]^2}{16L^2 \left[(d + 2\,(l + \varepsilon))^2 + 4x^2\right]} \right] . \tag{4.21}$$

- Joint between the null boundary of the WDW patch and the null boundary of the entanglement wedge anchored at RT_2 (curve G) with normals $\mathbf{k^+}$ and $\mathbf{w_2^+}$. The contribution gives

$$I_G = \frac{2L}{\pi G} \int_{x_{min}}^{x_{int}} dx \, \frac{d - 2\varepsilon}{4x^2 - (d - 2\varepsilon)^2} \log \left[\frac{\alpha \gamma \, (d - 2\varepsilon + 2x)^2 \, (d - 2\varepsilon - 2x)^2}{16L^2 \left[4x^2 + (d - 2\varepsilon)^2\right]} \right] . \tag{4.22}$$

16

4.4 Complexities

Adding up all the contributions and using polylog identities, we find:

$$\mathcal{C}_A^2 = \frac{c}{3\pi^2} \left\{ \log\left(\frac{\tilde{L}}{L}\right) \frac{l}{\varepsilon} - \log\left(\frac{2\tilde{L}}{L}\right) \log\left(\frac{d(d+2l)}{\varepsilon^2}\right) - \frac{\pi^2}{4} \right.$$
$$+ \left[\log\left(\frac{\tilde{L}}{L}\right) + \log\left(\frac{2(d+l)}{\sqrt{d(d+2l)}}\right) \right] \log\left(\frac{(d+l+\sqrt{d(d+2l)})^2}{l^2}\right) \qquad (4.23)$$
$$\left. + \mathrm{Li}_2\left(\frac{\sqrt{d(d+2l)}}{d+l}\right) - \mathrm{Li}_2\left(-\frac{\sqrt{d(d+2l)}}{d+l}\right) \right\} .$$

The spacetime volume complexity instead is

$$\mathcal{C}_{V2.0}^2 = \frac{2\,c}{3} \left\{ \frac{2l}{\varepsilon} - 2\log\frac{d(d+2l)}{\varepsilon^2} + \frac{\pi^2}{2} + 8\,\mathrm{arctanh}\sqrt{\frac{d}{d+2l}} \right.$$
$$\left. -2\left[\mathrm{Li}_2\left(\frac{\sqrt{d(d+2l)}}{d+l}\right) - \mathrm{Li}_2\left(-\frac{\sqrt{d(d+2l)}}{d+l}\right) \right] \right\} . \qquad (4.24)$$

The divergences of (4.23) and (4.24) are respectively the same as in eqs. (4.2); in particular, the subleading divergences are still poportional to the entanglement entropy

$$S = \frac{c}{3} \log \frac{d(d+2l)}{\varepsilon^2} . \qquad (4.25)$$

The finite part instead is a more complicated function of d, l compared to the single interval case.

5 Mutual complexity

Consider a physical system which is splitted into two sets A, B. The mutual information is defined as

$$I(A|B) = S(A) + S(B) - S(A \cup B). \qquad (5.1)$$

Since the entanglement entropy is shown to exhibit a subadditivity behaviour, *i.e.* the entanglement entropy of the full system is less than the sum of the entropies related to the two subsystems, the mutual information is a positive quantity.

Another quantity which measures the correlations between two physical subsystems was defined in [47, 58] and called *mutual complexity*:

$$\Delta\mathcal{C} = \mathcal{C}(\hat{\rho}_A) + \mathcal{C}(\hat{\rho}_B) - \mathcal{C}(\hat{\rho}_{A\cup B}). \qquad (5.2)$$

where $\hat{\rho}_A$, $\hat{\rho}_B$ are the reduced density matrices in the Hilbert spaces localised in A and B. If $\Delta\mathcal{C}$ is always positive, complexity is subadditive; if it is always negative, complexity is superadditive. By construction, in the CV and CV 2.0 conjectures complexity is always superadditive, i.e. $\Delta\mathcal{C} \leq 0$. Instead, in the CA conjecture, no general argument is known which fixes the sign of $\Delta\mathcal{C}$.

$\Delta\mathcal{C}$ is a finite quantity in all the three holographic conjectures. Moreover, $\Delta\mathcal{C} = 0$ for $d > d_0$ because in this case the RT surface is disconnected and then $\mathcal{C}(\hat{\rho}_A) + \mathcal{C}(\hat{\rho}_B) = \mathcal{C}(\hat{\rho}_{A\cup B})$. We will check that this quantity is generically discontinuous at $d = d_0$.

In the case of two disjoint intervals, from eq. (4.23) we find that the action mutual complexity is:

$$\Delta\mathcal{C}_A = \mathcal{C}_A^1 - \mathcal{C}_A^2 = \frac{c}{3\pi^2}\left\{\log\left(\frac{2\tilde{L}}{L}\right)\log\left(\frac{d(d+2l)}{l^2}\right) + \frac{\pi^2}{2}\right.$$
$$-\left[\log\left(\frac{\tilde{L}}{L}\right) + \log\left(\frac{2(d+l)}{\sqrt{d(d+2l)}}\right)\right]\log\left(\frac{(d+l+\sqrt{d(d+2l)})^2}{l^2}\right) \qquad (5.3)$$
$$\left.-\mathrm{Li}_2\left(\frac{\sqrt{d(d+2l)}}{d+l}\right) + \mathrm{Li}_2\left(-\frac{\sqrt{d(d+2l)}}{d+l}\right)\right\}.$$

The function $\Delta\mathcal{C}_A$ is plotted in figure 6 for various $\eta = \tilde{L}/L$. From the figure, we see that this quantity can be either positive or negative. At small d, the behavior of $\Delta\mathcal{C}_A$ is:

$$\Delta\mathcal{C}_A \approx \frac{c}{3\pi^2}\log\left(\frac{2\tilde{L}}{L}\right)\log\left(\frac{2d}{l}\right). \qquad (5.4)$$

For the value $\tilde{L}/L = 1/2$, the behaviour of $\Delta\mathcal{C}_A$ at $d \to 0$ switches from $-\infty$ to ∞.
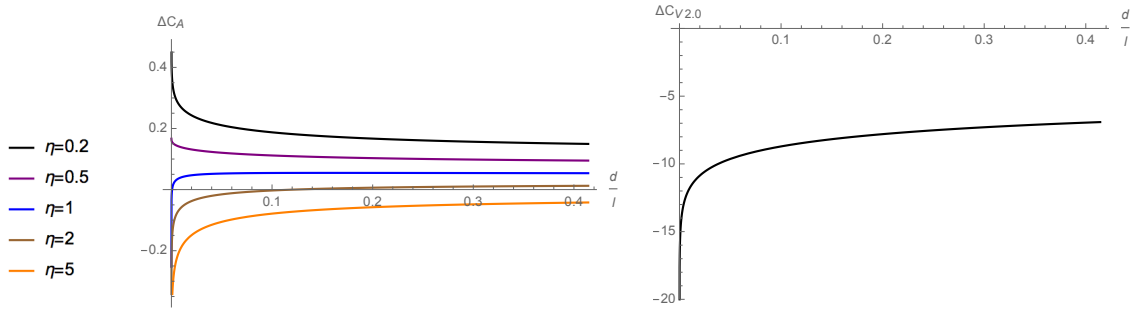

Figure 6: Left: Mutual complexity $\Delta\mathcal{C}_A$ for several values of $\eta = \tilde{L}/L$ as a function of $\frac{d}{l} \in [0, \frac{d_0}{l} = \sqrt{2} - 1]$. Right: Mutual complexity $\Delta\mathcal{C}_{V2.0}$. Here we set $c = 1$.

If $\eta \le 1/2$, CA is subadditive for all values of d/l. For $\eta > 1/2$, it is always possible to find small enough distances giving a superadditive behaviour. Moreover, there is a critical $\eta_0 \approx 2.465$ in such a way that complexity of two disjoint intervals is always superadditive if $\eta > \eta_0$. In order to have a positive definite subregion complexity, we should require $\eta > 1$. So it seems that it is not possible to achieve an universally subadditive complexity in a physically consistent setting.

A similar behaviour of subregion CA is found in the thermofield double state where the subsystems are taken as the two disconnected boundaries of spacetime. This case was investigated for asymptotically AdS black holes in D dimensions [46, 47], showing that the complexity=action is subadditive when $\eta < \hat{\eta}_D$ and superadditive for $\eta > \hat{\eta}_D$. The value of $\hat{\eta}_D$ is given by the zero of $g_D(\eta)$ [46]:

$$g_D(\eta) = \log((D-2)\eta) + \frac{1}{2}\left(\psi_0(1) - \psi_0\left(\frac{1}{D-1}\right)\right) + \frac{D-2}{D-1}\pi, \qquad (5.5)$$

where $\psi_0(z) = \Gamma'(z)/\Gamma(z)$ is the digamma function. For $D = 3$, $\hat{\eta}_3 \approx 0.1$.

In the CV 2.0 conjecture, from eq. (4.24) we find that the mutual complexity for two

disjoint intervals is:

$$\Delta \mathcal{C}_{V2.0} = \mathcal{C}^1_{V2.0} - \mathcal{C}^2_{V2.0} = \frac{4\,c}{3} \left[\log \frac{d(d+2l)}{l^2} - \frac{\pi^2}{2} - 4\operatorname{arctanh} \sqrt{\frac{d}{d+2l}} \right.$$
$$\left. + \operatorname{Li}_2 \left(\frac{\sqrt{d(d+2l)}}{d+l} \right) - \operatorname{Li}_2 \left(-\frac{\sqrt{d(d+2l)}}{d+l} \right) \right] , \tag{5.6}$$

see figure 6 for a plot. This is negative definite as expected, because the bulk region involved in the first configuration of RT surface is smaller than the second region.

In the CV conjecture, we can use eqs. (3.33) and (3.34) from [44] to determine mutual complexity. Considering the case of a double segment, we find that for $d < d_0$ the mutual complexity is constant:

$$\Delta \mathcal{C}_V = -\frac{4\,c}{3}\pi\,. \tag{5.7}$$

5.1 Strong super/subaddivity for overlapping segments

Given two generically overlapping regions A and B, entanglement entropy satisfies the strong subadditivity property:

$$\tilde{\Delta} S = S(A) + S(B) - S(A \cup B) - S(A \cap B) \geq 0\,. \tag{5.8}$$

Inspired by this relation, we can define [58] by analogy a generalization of the mutual complexity as:

$$\tilde{\Delta} \mathcal{C}(A, B) = \mathcal{C}(\hat{\rho}_A) + \mathcal{C}(\hat{\rho}_B) - \mathcal{C}(\hat{\rho}_{A\cup B}) - \mathcal{C}(\hat{\rho}_{A\cap B})\,. \tag{5.9}$$

This definition generalizes eq. (5.2) to the case where $A \cap B \neq \emptyset$. We can investigate the sign of this quantity in the case of two overlapping segments.

Suppose that we consider the regions given by two intervals of lengths a, b which intersect in a segment of length c. The union of these intervals is a segment of total length $a + b - c$. From eqs. (3.29) and (3.30), we find

$$\tilde{\Delta} \mathcal{C}_A^{\mathrm{BTZ}} = -\log \left(\frac{2\tilde{L}}{L} \right) \tilde{\Delta} S^{\mathrm{BTZ}}\,,$$
$$\tilde{\Delta} \mathcal{C}_{V2.0}^{\mathrm{BTZ}} = -4\tilde{\Delta} S^{\mathrm{BTZ}}\,, \tag{5.10}$$

where $\tilde{\Delta} S^{\mathrm{BTZ}}$ is the quantity defined in (5.8), computed for the two overlapping intervals in the BTZ background. Then $\mathcal{C}_A$ is strongly subadditive for $\tilde{L}/L < 1/2$ and strongly superadditive for $\tilde{L}/L > 1/2$. Instead $\mathcal{C}_{V2.0}$ is strongly superadditive.

6 Conclusions

We studied the CA and CV 2.0 subregion complexity conjectures in AdS$_3$ and in the BTZ background. The main results of this paper are:

- In the case of one segment, we find that subregion complexity for AdS$_3$ and for the BTZ can be directly related to the entanglement entropy, see eqs. (1.4) and (3.30).

- In the case of a two segments subregion, complexity in AdS$_3$ is a more complicated function of the lengths and the relative separation of the segments, see eqs. (4.23) and (4.24). Subregion complexity carries a different amount of information compared to the entanglement entropy. In particular, for two disjoint segments the mutual complexity (defined in eq. (5.2)) is not proportional to mutual information.

One of the obscure aspects of the CA conjecture is the physical meaning of the scale $\tilde{L}$ appearing in the action counterterm eq. (2.19) on the null boundaries. A deeper understanding of the role of this parameter is desirable. In particular, its relation with the field theory side of the correspondence remains completely unclear.

We find that the sign of action mutual complexity $\Delta\mathcal{C}_A$ of a two disjoint segments subregion depends drastically on $\eta = \tilde{L}/L$ (see figure 6):

- For $\eta \geq \eta_0 \approx 2.465$, $\Delta\mathcal{C}_A$ is always negative, and so $\mathcal{C}_A$ is superadditive as $\mathcal{C}_V$ and $\mathcal{C}_{V2.0}$.

- For $\frac{1}{2} < \eta < \eta_0$, $\Delta\mathcal{C}_A$ is negative at small d and positive at large d. This region should be partially unphysical, because in order to obtain a positive-definite $\mathcal{C}_A$, we have to require $\tilde{L} > L$ and so $\eta > 1$.

- In the unphysical region $0 < \eta \leq 1/2$, action complexity is subadditive.

It would be interesting to study the case of higher dimensional AdS space, in order to investigate the behaviour of mutual complexity for regions of different shape, such as a higher dimensional spheres or strips.

In the CV conjecture, subregion complexity for multiple intervals in the BTZ background is independent of temperature and can be computed using topology from the Gauss-Bonnet theorem, see [44]. It would be interesting to investigate if a similar relation with topology holds also for CA and CV 2.0. The complicated structure of the finite terms in eqs. (4.23) and (4.24) suggests that such relation, if exists, is more intricated than in CV.

Acknowledgments

Appendix

A Another regularization for the action of one segment in BTZ

In this Appendix we follow another prescription to regularize the action where the null boundaries of the WDW patch are sent from the true boundary $z = 0$ and we add a timelike cutoff surface at $z = \varepsilon$ cutting the bulk structure we integrate over. The geometry of the region is shown in figure 7.

The geometric data are slightly different than the ones introduced in Section 3. The RT surface and the corresponding entanglement wedge are the same, see eqs. (3.3) and (3.8). The WDW patch starts from the true boundary $z = 0$ and then the null lines which delimit it are parametrized by

$$t_{\text{WDW}} = \pm \frac{z_h}{4} \log \left(\frac{z_h + z}{z_h - z} \right)^2 , \tag{A.1}$$

where $\pm$ refers to positive and negative times, respectively. The intersection curve between the WDW patch and the entanglement wedge is given by

$$z_{\text{int}} = \coth \left(\frac{l}{2 z_h} \right) - \cosh \left(\frac{x}{z_h} \right) \operatorname{csch} \left(\frac{l}{2 z_h} \right) . \tag{A.2}$$
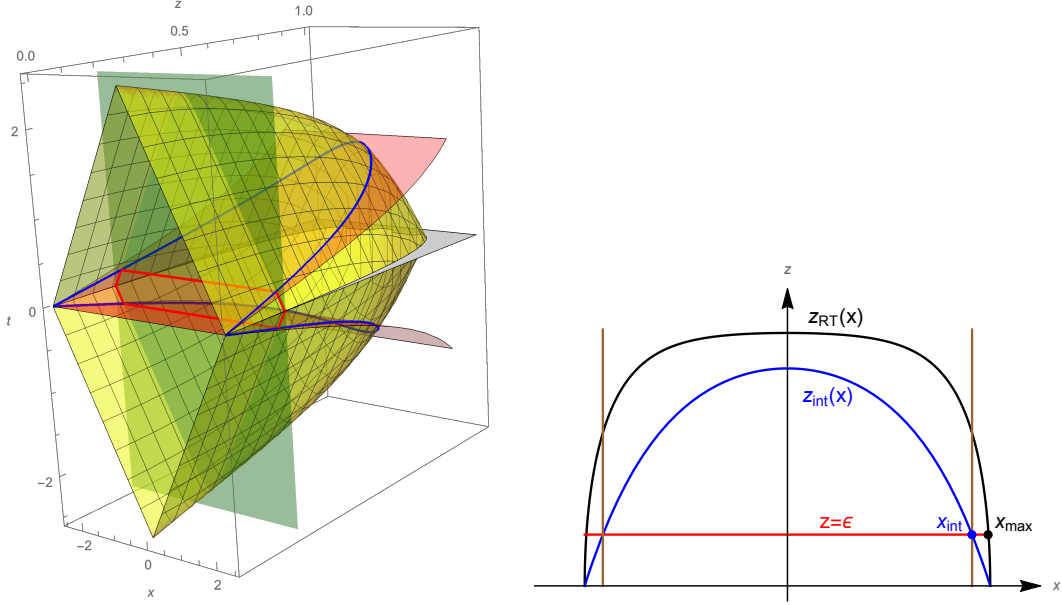
Figure 7: Another regularization for the BTZ case.

The null normals to the boundaries of the WDW patch and the entanglement wedge are unchanged.

Unlike the case of the other regularization, the intersection curve and the RT surface do not meet at $z = \varepsilon$, but at the true boundary $z = 0$. For this region, there are no codimension-3 joints. The intersection curve between the boundaries of the WDW patch and the entanglement wedge meets the cutoff surface at:

$$x_{\text{int}} = \text{arccosh} \left[\cosh \left(\frac{l}{2z_h} \right) - \frac{\varepsilon}{z_h} \sinh \left(\frac{l}{2z_h} \right) \right] . \tag{A.3}$$

This expression is found by inverting eq. (A.2) and imposing $z = \varepsilon$. In the folowing sections we compute all the terms entering the gravitational action.

A.1 Bulk contribution

We split the contributions as follows

$$I_{\text{bulk}} = 4 \left(I_{\text{bulk}}^1 + I_{\text{bulk}}^2 + I_{\text{bulk}}^3 \right) , \tag{A.4}$$

where

$$
\begin{aligned}
I_{\text{bulk}}^1 &= -\frac{L}{4\pi G} \int_0^{x_{\text{int}}} dx \int_\varepsilon^{z_{\text{int}}} dz \int_0^{t_{\text{WDW}}} dt \, \frac{1}{z^3} , \\
I_{\text{bulk}}^2 &= -\frac{L}{4\pi G} \int_0^{x_{\text{int}}} dx \int_{z_{\text{int}}}^{z_{\text{RT}}} dz \int_0^{t_{\text{EW}}} dt \, \frac{1}{z^3} , \\
I_{\text{bulk}}^3 &= -\frac{L}{4\pi G} \int_{x_{\text{int}}}^{x_{\text{max}}} dx \int_\varepsilon^{z_{\text{RT}}} dz \int_0^{t_{\text{EW}}} dt \, \frac{1}{z^3} .
\end{aligned}
\tag{A.5}
$$

In this case the sum of bulk terms obtained by splitting the spacetime region with the intersection between the boundaries of the WDW patch and the entanglement wedge does not give the entire bulk action. We need to add I_{bulk}^3 which accounts for the region between the values x_{int} and x_{max} of the transverse coordinate.

A direct evaluation gives

$$I_{\text{bulk}}^1 + I_{\text{bulk}}^2 = \frac{L}{16\pi G z_h} \int_0^{x_{\text{int}}(\varepsilon)} dx \left\{ \coth\left(\frac{x}{z_h}\right) \log \left| \frac{\sinh\left(\frac{l-2x}{2z_h}\right) \sinh^2\left[\frac{l+2x}{4z_h}\right]}{\sinh\left(\frac{l+2x}{2z_h}\right) \sinh^2\left[\frac{l-2x}{4z_h}\right]} \right| \right.$$
$$\left. + \frac{2\sinh\left(\frac{l}{2z_h}\right)}{\cosh\left(\frac{l}{2z_h} - \cosh\left(\frac{x}{z_h}\right)\right)} - \frac{2z_h}{\varepsilon} + \left(\frac{z_h^2}{\varepsilon^2} - 1\right) \log\left|\frac{z_h - \varepsilon}{z_h + \varepsilon}\right| \right\} . \tag{A.6}$$

$$I_{\text{bulk}}^3 = -\frac{L}{16\pi G} . \tag{A.7}$$

A.2 Gibbons-Hawking-York contribution

The Gibbons-Hawking-York (GHY) surface term in the action for timelike and spacelike boundaries is

$$I_{GHY} = \frac{1}{8\pi G} \int_{\partial \mathcal{B}'} d^2x \sqrt{-\det h_{\mu\nu}} \, K \tag{A.8}$$

with $h_{\mu\nu}$ the induced metric on the boundary and K the trace of the extrinsic curvature. The only contribution of this kind comes from the timelike regularizing surface at $z = \varepsilon$.

The GHY contribution is given by two parts. The first one involves the WDW patch, while the second one involves the entanglement wedge:

$$I_{\text{GHY}}^1 = \left[\frac{L}{8\pi G} \int_0^{x_{\text{int}}} dx \int_0^{t_{\text{WDW}}} dt \left(\frac{2}{z^2} - \frac{1}{z_h^2}\right) \right]_{z=\varepsilon} = \frac{L}{8\pi G} \frac{l}{\varepsilon} - \frac{L}{4\pi G} , \tag{A.9}$$

$$I_{\text{GHY}}^2 = \left[\frac{L}{8\pi G} \int_{x_{\text{int}}}^{x_{max}} dx \int_0^{t_{\text{EW}}} dt \left(\frac{2}{z^2} - \frac{1}{z_h^2}\right) \right]_{z=\varepsilon} = \frac{L}{8\pi G} . \tag{A.10}$$

The total GHY contribution is

$$I_{\text{GHY}} = 4 \left(I_{\text{GHY}}^1 + I_{\text{GHY}}^2 \right) = \frac{L}{2\pi G} \left(\frac{l}{\varepsilon} - 1\right) . \tag{A.11}$$

A.3 Null boundaries counterterms

The details of calculation are very similar to the ones in section 3.3. The contribution in eq. (2.15) and the counterterm on the boundary of entanglement wedge again vanish. The counterterm on the boundary of the WDW patch gives:

$$I_{\text{ct}}^{\text{WDW}} = -\frac{L}{2\pi G} \int_0^{x_{\text{int}}} dx \int_\varepsilon^{z_{\text{int}}} dz \frac{1}{z^2} \log\left|\frac{\tilde{L}}{L^2} \alpha z\right| =$$
$$= \frac{L}{2\pi G} \int_0^{x_{\text{max}}} dx \left\{ \frac{1 + \log\left|\frac{\tilde{L}}{L^2}\alpha\varepsilon\right|}{\varepsilon} + \frac{\sinh\left(\frac{l}{2z_h}\right)}{z_h\left[\cosh\left(\frac{x}{z_h}\right) - \cosh\left(\frac{l}{2z_h}\right)\right]} \times \right.$$
$$\left. \times \left(1 + \log\left|\frac{\tilde{L}z_h\alpha}{L^2} \frac{\cosh\left(\frac{l}{2z_h}\right) - \cosh\left(\frac{x}{z_h}\right)}{\cosh\left(\frac{l}{2z_h}\right)}\right|\right) \right\} . \tag{A.12}$$

A.4 Joint terms

The joint contribution to the gravitational action coming from a codimension-2 surface given by the intersection of a codimension-1 null surface and a codimension-1 timelike (or spacelike) surface is

$$I_{\mathcal{J}} = \frac{\eta}{8\pi G} \int_{\mathcal{J}} dx \sqrt{\sigma} \log |\mathbf{k} \cdot \mathbf{n}| \,, \tag{A.13}$$

where σ is the induced metric determinant on the codimension-2 surface and $\mathbf{n}$ and $\mathbf{k}$ are the outward-directed normals to the timelike (or spacelike) surface and the null one respectively. Moreover,

$$\eta = -\operatorname{sign}(\mathbf{k} \cdot \mathbf{n}) \operatorname{sign}(\mathbf{k} \cdot \hat{t}) \tag{A.14}$$

in which $\hat{t}$ is the auxiliary unit vector in the tangent space of the boundary region, orthogonal to the joint and outward-directed from the region of interest [42].

The unit normal vector n^{μ} to the $z = \varepsilon$ surface is

$$n^{\mu} = \left(0, -\frac{z}{L}\sqrt{f(z)}, 0\right) \tag{A.15}$$

where the sign must be chosen so that the vector is outward-directed from the region of interest.

The joints give the following contributions:

- The joint involving the WDW patch boundary and the cutoff surface:

$$I_{\mathcal{J}}^{\mathrm{cutoff1}} = -\frac{L}{2\pi G} \int_0^{x_{\mathrm{int}}} \frac{dx}{\varepsilon} \log\left(\frac{\alpha\,\varepsilon}{L\sqrt{f(\varepsilon)}}\right) = -\frac{L}{4\pi G}\frac{l}{\varepsilon}\log\left(\frac{L}{\alpha\varepsilon}\right) - \frac{L}{2\pi G}\log\left(\frac{L}{\alpha\varepsilon}\right). \tag{A.16}$$

- Next we consider the joint involving the cutoff surface and the entanglement wedge boundary:

$$I_{\mathcal{J}}^{\mathrm{cutoff2}} = \mathcal{O}\left(\varepsilon \log \varepsilon\right). \tag{A.17}$$

- The null-null joint contribution coming from the RT surface is the same as in the previous regularization, see eq. (3.24).

- The joints coming from the intersection between the null boundaries of the WDW patch and the ones of the entanglement wedge give a similar contribution as in eq. (3.25), The main difference is that the integral is in the range $[0, x_{\mathrm{int}}(\varepsilon)]$ and the intersection is slightly different, because the WDW patch starts from $z = 0$ in the present regularization:

$$I_{\mathcal{J}}^{\mathrm{int}} = \frac{L}{2\pi G z_h} \int_0^{x_{\mathrm{int}}} dx \frac{\sinh\left(\frac{l}{2z_h}\right)}{\cosh\left(\frac{l}{2z_h}\right) - \cosh\left(\frac{x}{z_h}\right)} \log\left|\frac{\alpha\beta z_h^2}{2L^2} \frac{\left(\cosh\left(\frac{l}{2z_h}\right) - \cosh\left(\frac{x}{z_h}\right)\right)^2}{\cosh\left(\frac{x}{z_h}\right)\cosh\left(\frac{l}{2z_h}\right) - 1}\right|. \tag{A.18}$$

A.5 Complexity

Adding all the contributions and performing the integrals we finally get

$$\mathcal{C}_A^{\mathrm{BTZ}} = \frac{l}{\varepsilon}\frac{c}{6\pi^2}\left(1 + \log\left(\frac{\tilde{L}}{L}\right)\right) - \log\left(\frac{2\tilde{L}}{L}\right)\frac{S^{\mathrm{BTZ}}}{\pi^2} - \frac{c}{3\pi^2}\left(\frac{1}{2} + \log\left(\frac{\tilde{L}}{L}\right)\right) + \frac{1}{24}c. \tag{A.19}$$

The difference with expression (3.29) consists only in the coefficient of the divergence $1/\varepsilon$ and in a finite piece proportional to the counterterm scale $\tilde{L}$ via a logarithm.

Recently other counterterms were proposed to give a universal behaviour of all the divergences of the action [64]. In particular, with this regularization we need to insert a codimension-1 boundary term at the cutoff surface:

$$I_{\text{ct}}^{\text{cutoff}} = -\frac{1}{16\pi G} \int d^{d-1}x\, dt\, \sqrt{-h} \left(\frac{2(d-1)}{L} + \frac{L}{d-2}\tilde{R} \right), \qquad (A.20)$$

being $\tilde{R}$ the Ricci scalar on the codimension-1 surface. Adding the extra counterterm in eq. (A.20), we find

$$\mathcal{C}_A^{\text{BTZ}} = \frac{l}{\varepsilon}\frac{c}{6\pi^2} \log\left(\frac{\tilde{L}}{L}\right) - \log\left(\frac{2\tilde{L}}{L}\right)\frac{S^{\text{BTZ}}}{\pi^2} - \frac{c}{3\pi^2}\log\left(\frac{\tilde{L}}{L}\right) + \frac{1}{24}c. \qquad (A.21)$$

The numerical coefficient of all the divergences is the same as in eq. (3.29). The two regularizations differ only by a finite piece dependent from the counterterm length scale $\tilde{L}$.

References

[1] S. Ryu and T. Takayanagi, Phys. Rev. Lett. **96** (2006) 181602 doi:10.1103/PhysRevLett.96.181602 [hep-th/0603001].

[2] J. D. Bekenstein, Phys. Rev. D **7** (1973) 2333. doi:10.1103/PhysRevD.7.2333

[3] M. Rangamani and T. Takayanagi, Lect. Notes Phys. **931** (2017) pp.1 doi:10.1007/978-3-319-52573-0 [arXiv:1609.01287 [hep-th]].

[4] M. Headrick, arXiv:1907.08126 [hep-th].

[5] L. Susskind, [Fortsch. Phys. **64** (2016) 24] Addendum: Fortsch. Phys. **64** (2016) 44 doi:10.1002/prop.201500093, 10.1002/prop.201500092 [arXiv:1403.5695 [hep-th], arXiv:1402.5674 [hep-th]].

[6] D. Stanford and L. Susskind, Phys. Rev. D **90** (2014) no.12, 126007 doi:10.1103/PhysRevD.90.126007 [arXiv:1406.2678 [hep-th]].

[7] L. Susskind, Fortsch. Phys. **64** (2016) 49 doi:10.1002/prop.201500095 [arXiv:1411.0690 [hep-th]].

[8] L. Susskind, arXiv:1810.11563 [hep-th].

[9] Michael A. Nielsen, Quantum Information & Computation, Volume 6 Issue 3, May 2006, Pages 213-262, [arXiv:quant-ph/0502070]

[10] Mark R. Dowling, Michael A. Nielsen, Quantum Information & Computation, Volume 8 Issue 10, November 2008, Pages 861-899, [arXiv:quant-ph/0701004]

[11] R. Jefferson and R. C. Myers, JHEP **1710** (2017) 107 doi:10.1007/JHEP10(2017)107 [arXiv:1707.08570 [hep-th]].

[12] S. Chapman, M. P. Heller, H. Marrochio and F. Pastawski, Phys. Rev. Lett. **120** (2018) no.12, 121602 doi:10.1103/PhysRevLett.120.121602 [arXiv:1707.08582 [hep-th]].

[13] K. Hashimoto, N. Iizuka and S. Sugishita, Phys. Rev. D **96** (2017) no.12, 126001 doi:10.1103/PhysRevD.96.126001 [arXiv:1707.03840 [hep-th]].

[14] S. Chapman, J. Eisert, L. Hackl, M. P. Heller, R. Jefferson, H. Marrochio and R. C. Myers, SciPost Phys. **6** (2019) no.3, 034 doi:10.21468/SciPostPhys.6.3.034 [arXiv:1810.05151 [hep-th]].

[15] P. Caputa, N. Kundu, M. Miyaji, T. Takayanagi and K. Watanabe, Phys. Rev. Lett. **119** (2017) no.7, 071602 doi:10.1103/PhysRevLett.119.071602 [arXiv:1703.00456 [hep-th]].

[16] P. Caputa, N. Kundu, M. Miyaji, T. Takayanagi and K. Watanabe, JHEP **1711** (2017) 097 doi:10.1007/JHEP11(2017)097 [arXiv:1706.07056 [hep-th]].

[17] A. Bhattacharyya, P. Caputa, S. R. Das, N. Kundu, M. Miyaji and T. Takayanagi, arXiv:1804.01999 [hep-th].

[18] A. R. Brown, D. A. Roberts, L. Susskind, B. Swingle and Y. Zhao, Phys. Rev. Lett. **116** (2016) no.19, 191301 doi:10.1103/PhysRevLett.116.191301 [arXiv:1509.07876 [hep-th]].

[19] A. R. Brown, D. A. Roberts, L. Susskind, B. Swingle and Y. Zhao, Phys. Rev. D **93** (2016) no.8, 086006 doi:10.1103/PhysRevD.93.086006 [arXiv:1512.04993 [hep-th]].

[20] J. Couch, W. Fischler and P. H. Nguyen, JHEP **1703** (2017) 119 doi:10.1007/JHEP03(2017)119 [arXiv:1610.02038 [hep-th]].

[21] L. Lehner, R. C. Myers, E. Poisson and R. D. Sorkin, Phys. Rev. D **94** (2016) no.8, 084046 doi:10.1103/PhysRevD.94.084046 [arXiv:1609.00207 [hep-th]].

[22] R. G. Cai, S. M. Ruan, S. J. Wang, R. Q. Yang and R. H. Peng, JHEP **1609** (2016) 161 doi:10.1007/JHEP09(2016)161 [arXiv:1606.08307 [gr-qc]].

[23] S. Chapman, H. Marrochio and R. C. Myers, JHEP **1701** (2017) 062 doi:10.1007/JHEP01(2017)062 [arXiv:1610.08063 [hep-th]].

[24] D. Carmi, S. Chapman, H. Marrochio, R. C. Myers and S. Sugishita, JHEP **1711** (2017) 188 doi:10.1007/JHEP11(2017)188 [arXiv:1709.10184 [hep-th]].

[25] S. Chapman, D. Ge and G. Policastro, JHEP **1905** (2019) 049 doi:10.1007/JHEP05(2019)049 [arXiv:1811.12549 [hep-th]].

[26] M. Moosa, JHEP **1803** (2018) 031 doi:10.1007/JHEP03(2018)031 [arXiv:1711.02668 [hep-th]].

[27] M. Moosa, Phys. Rev. D **97** (2018) no.10, 106016 doi:10.1103/PhysRevD.97.106016 [arXiv:1712.07137 [hep-th]].

[28] S. Chapman, H. Marrochio and R. C. Myers, JHEP **1806** (2018) 046 doi:10.1007/JHEP06(2018)046 [arXiv:1804.07410 [hep-th]].

[29] S. Chapman, H. Marrochio and R. C. Myers, JHEP **1806** (2018) 114 doi:10.1007/JHEP06(2018)114 [arXiv:1805.07262 [hep-th]].

[30] J. L. F. Barbon and E. Rabinovici, JHEP **1601** (2016) 084 doi:10.1007/JHEP01(2016)084 [arXiv:1509.09291 [hep-th]].

[31] S. Bolognesi, E. Rabinovici and S. R. Roy, JHEP **1806** (2018) 016 doi:10.1007/JHEP06(2018)016 [arXiv:1802.02045 [hep-th]].

[32] M. Flory and N. Miekley, JHEP **1905** (2019) 003 doi:10.1007/JHEP05(2019)003 [arXiv:1806.08376 [hep-th]].

[33] M. Flory, JHEP **1905** (2019) 086 doi:10.1007/JHEP05(2019)086 [arXiv:1902.06499 [hep-th]].

[34] M. Alishahiha, A. Faraji Astaneh, M. R. Mohammadi Mozaffar and A. Mollabashi, JHEP **1807** (2018) 042 doi:10.1007/JHEP07(2018)042 [arXiv:1802.06740 [hep-th]].

[35] M. Ghodrati, Phys. Rev. D **96** (2017) no.10, 106020 doi:10.1103/PhysRevD.96.106020 [arXiv:1708.07981 [hep-th]].

[36] R. Auzzi, S. Baiguera and G. Nardelli, JHEP **1806** (2018) 063 doi:10.1007/JHEP06(2018)063 [arXiv:1804.07521 [hep-th]].

[37] R. Auzzi, S. Baiguera, M. Grassi, G. Nardelli and N. Zenoni, JHEP **1809** (2018) 013 doi:10.1007/JHEP09(2018)013 [arXiv:1806.06216 [hep-th]].

[38] H. Dimov, R. C. Rashkov and T. Vetsov, Phys. Rev. D **99** (2019) no.12, 126007 doi:10.1103/PhysRevD.99.126007 [arXiv:1902.02433 [hep-th]].

[39] M. Headrick, V. E. Hubeny, A. Lawrence and M. Rangamani, JHEP **1412** (2014) 162 doi:10.1007/JHEP12(2014)162 [arXiv:1408.6300 [hep-th]].

[40] M. Alishahiha, Phys. Rev. D **92** (2015) no.12, 126009 doi:10.1103/PhysRevD.92.126009 [arXiv:1509.06614 [hep-th]].

[41] V. E. Hubeny, M. Rangamani and T. Takayanagi, JHEP **0707** (2007) 062 doi:10.1088/1126-6708/2007/07/062 [arXiv:0705.0016 [hep-th]].

[42] D. Carmi, R. C. Myers and P. Rath, JHEP **1703** (2017) 118 doi:10.1007/JHEP03(2017)118 [arXiv:1612.00433 [hep-th]].

[43] O. Ben-Ami and D. Carmi, JHEP **1611** (2016) 129 doi:10.1007/JHEP11(2016)129 [arXiv:1609.02514 [hep-th]].

[44] R. Abt, J. Erdmenger, H. Hinrichsen, C. M. Melby-Thompson, R. Meyer, C. Northe and I. A. Reyes, Fortsch. Phys. **66** (2018) no.6, 1800034 doi:10.1002/prop.201800034 [arXiv:1710.01327 [hep-th]].

[45] R. Abt, J. Erdmenger, M. Gerbershagen, C. M. Melby-Thompson and C. Northe, JHEP **1901** (2019) 012 doi:10.1007/JHEP01(2019)012 [arXiv:1805.10298 [hep-th]].

[46] C. A. Agón, M. Headrick and B. Swingle, JHEP **1902** (2019) 145 doi:10.1007/JHEP02(2019)145 [arXiv:1804.01561 [hep-th]].

[47] M. Alishahiha, K. Babaei Velni and M. R. Mohammadi Mozaffar, Phys. Rev. D **99** (2019) no.12, 126016 doi:10.1103/PhysRevD.99.126016 [arXiv:1809.06031 [hep-th]].

[48] E. Cáceres, J. Couch, S. Eccles and W. Fischler, Phys. Rev. D **99** (2019) no.8, 086016 doi:10.1103/PhysRevD.99.086016 [arXiv:1811.10650 [hep-th]].

[49] P. Roy and T. Sarkar, Phys. Rev. D **96** (2017) no.2, 026022 doi:10.1103/PhysRevD.96.026022 [arXiv:1701.05489 [hep-th]].

[50] P. Roy and T. Sarkar, Phys. Rev. D **97** (2018) no.8, 086018 doi:10.1103/PhysRevD.97.086018 [arXiv:1708.05313 [hep-th]].

[51] E. Bakhshaei, A. Mollabashi and A. Shirzad, Eur. Phys. J. C **77** (2017) no.10, 665 doi:10.1140/epjc/s10052-017-5247-1 [arXiv:1703.03469 [hep-th]].

[52] A. Bhattacharya, K. T. Grosvenor and S. Roy, arXiv:1905.02220 [hep-th].

[53] R. Auzzi, S. Baiguera, A. Mitra, G. Nardelli and N. Zenoni, arXiv:1906.09345 [hep-th].

[54] B. Chen, W. M. Li, R. Q. Yang, C. Y. Zhang and S. J. Zhang, JHEP **1807** (2018) 034 doi:10.1007/JHEP07(2018)034 [arXiv:1803.06680 [hep-th]].

[55] R. Auzzi, G. Nardelli, F. I. Schaposnik Massolo, G. Tallarita and N. Zenoni, arXiv:1908.10832 [hep-th].

[56] M. Banados, C. Teitelboim and J. Zanelli, Phys. Rev. Lett. **69** (1992) 1849 doi:10.1103/PhysRevLett.69.1849 [hep-th/9204099].

[57] M. Banados, M. Henneaux, C. Teitelboim and J. Zanelli, Phys. Rev. D **48** (1993) 1506 Erratum: [Phys. Rev. D **88** (2013) 069902] doi:10.1103/PhysRevD.48.1506, 10.1103/PhysRevD.88.069902 [gr-qc/9302012].

[58] E. Caceres, S. Chapman, J. D. Couch, J. P. Hernandez, R. C. Myers and S. M. Ruan, arXiv:1909.10557 [hep-th].

[59] E. Poisson, "A Relativist's Toolkit: The Mathematics of Black-Hole Mechanics," doi:10.1017/CBO9780511606601

[60] B. Czech, J. L. Karczmarek, F. Nogueira and M. Van Raamsdonk, Class. Quant. Grav. **29** (2012) 155009 doi:10.1088/0264-9381/29/15/155009 [arXiv:1204.1330 [hep-th]].

[61] V. E. Hubeny and M. Rangamani, JHEP **1206** (2012) 114 doi:10.1007/JHEP06(2012)114 [arXiv:1204.1698 [hep-th]].

[62] A. C. Wall, Class. Quant. Grav. **31** (2014) no.22, 225007 doi:10.1088/0264-9381/31/22/225007 [arXiv:1211.3494 [hep-th]].

[63] V. Balasubramanian *et al.*, Phys. Rev. D **84** (2011) 026010 doi:10.1103/PhysRevD.84.026010 [arXiv:1103.2683 [hep-th]].

[64] A. Akhavan and F. Omidi, arXiv:1906.09561 [hep-th].